

Benefit and cost of siderophores

We determined that siderophore production is an appropriate cooperative trait for our experiment. We measured the growth rates of a wild-type strain that produces the primary siderophore, pyoverdinin (cooperator), and a mutant strain that does not (cheater), either when alone or in mixed cultures where the other strain was present, and at a variety of iron availabilities. Both strains were grown overnight in 30 ml glass universals containing 6 ml standard King's medium B (KB) in an orbital shaker (200 r.p.m.), at 37 °C. Cell densities did not differ between strains when grown under these conditions ($n = 12$, 2-sample t -test: $t = 0.37$, $P > 0.2$). Sixteen universals containing Casamino acids medium (CAA; 5 g Casamino acids, 1.18 g $K_2HPO_4 \cdot 3H_2O$, 0.25 g $MgSO_4 \cdot 7H_2O$, per litre) media were inoculated with 10^6 overnight culture cells of either PA01, PA6609 or a 50:50 mixture of both, resulting in a total of 48 cultures. Sodium bicarbonate was added to each tube to create a 20 mM solution, necessary for effective chelator activity²⁷. Four tubes inoculated with the three different bacterial populations (PA01, PA6609 and both) were exposed to three different iron-limitation treatments: 50 $\mu g ml^{-1}$, 100 $\mu g ml^{-1}$ and 200 $\mu g ml^{-1}$ of human apo-transferrin (Sigma), a natural iron-chelator, were added. Human iron chelators (such as transferrin) bind iron, preventing non-siderophore-mediated uptake of iron by bacteria. Siderophores are also strong iron chelators, and so compete with transferrin for iron. The tubes were incubated at 37 °C in a static incubator for 24 h. Cultures were then plated onto KB agar and relative densities were determined.

Siderophore (pyoverdinin) production in these strains has the characteristics that make an appropriate cooperative trait for our study. First, there is a cost to individuals that can produce pyoverdinin, as shown by monocultures of mutants being able to outcompete wild-type strains in an iron-rich environment ($F_{(1,6)} = 12.61$, $P = 0.01$). Second, when iron is limiting, siderophore production is beneficial, as shown by populations containing wild-type strains growing to a higher density than those where pyoverdinin producers are absent ($F_{(1,21)} = 16.13$, $P = 0.0006$). Chelator concentration was also significant ($F_{(1,21)} = 12.45$, $P = 0.002$), but not the interaction ($F_{(1,20)} = 0.69$, $P = 0.42$). Third, individuals who do not produce pyoverdinin are able to exploit the pyoverdinin produced by the others, as shown by mutants growing to higher densities in the presence of wild type in iron-poor environments ($t = 6.37$, d.f. = 10, $P < 0.005$). Consequently, pyoverdinin production is a costly altruistic trait that can potentially be exploited by cheaters.

Selection experiment

We independently manipulated relatedness and the scale of competition, using a classic two factorial ANOVA design. Replicates contained one population divided into 12 subpopulations. Each subpopulation was grown in a tube of CAA medium supplemented with 20 mM $NaHCO_3$ and 100 $\mu g ml^{-1}$ human apo-transferrin²⁷. In high relatedness treatments, six tubes were inoculated with 10^6 cells from an overnight culture of either PA01 or PA6609 (1:1 overall ratio of altruist to cheater). Low relatedness treatments initially comprised 12 tubes inoculated with 10^6 cells of a 1:1 mix of both strains. Cultures were then grown for 24 h in a 37 °C static incubator, during which time approximately seven generations take place. Local competition cultures were then individually plated onto KB agar, whereas an equal volume from each culture within a global competition treatment were mixed together before plating. Plates were incubated for 24 h at 37 °C, and after determining relative frequencies of the two strains, 24 or 12 (low and high relatedness treatments, respectively) random colonies were separately inoculated into KB media and grown at 200 r.p.m. and 37 °C, overnight. CAA tubes were then inoculated with a total of 10^6 cells from these overnight cultures: low relatedness tubes were inoculated with one clone, and high relatedness with two. (Colonies were grown up in KB rather than used to inoculate the subsequent transfer directly, to control for the difference in size between altruistic and cheater colonies, and therefore starting densities). This selection procedure was repeated for six transfers, allowing a total of 42 (7 × 6) bacterial generations under experimental conditions. Every round of selection we counted the frequencies of altruistic and selfish bacteria growing on the agar plates, and the relative proportion inoculated into the next round. We used the proportion of cooperators inoculated into the next generation as the response variable in our analyses, and in Fig. 3. The whole experiment was repeated a further three times.

Analyses

We analysed our data using standard ANOVA methodology, as implemented in the package GLMStat 5.7.5 (Kagi Shareware). For all analyses on the proportion of cheaters (pyoverdinin-minus colonies) in the population, the proportion was arcsine square root transformed before analysis, and a normal distribution subsequently confirmed with a Shapiro-Wilkinson test. We present the analyses for the end of the experiment after six transfers.

Received 26 April; accepted 11 June 2004; doi:10.1038/nature02744.

1. Maynard Smith, J. & Szathmari, E. *The Major Transitions in Evolution* (W.H. Freeman, Oxford, 1995).
2. Hamilton, W. D. *Narrow Roads of Gene Land: I Evolution of Social Behaviour* (W.H. Freeman, Oxford, 1996).
3. Frank, S. A. *Foundations of Social Evolution* (Princeton Univ. Press, Princeton, 1998).
4. Hamilton, W. D. The evolution of altruistic behaviour. *Am. Nat.* **97**, 354–356 (1963).
5. Hamilton, W. D. The genetical evolution of social behaviour, I & II. *J. Theor. Biol.* **7**, 1–52 (1964).
6. Crespi, B. J. The evolution of social behavior in microorganisms. *Trends Ecol. Evol.* **16**, 178–183 (2001).
7. Keller, L. & Reeve, H. K. In *Encyclopedia of Evolution* (ed. Pagel, M. D.) 595–600 (Oxford Univ. Press, Oxford, 2002).
8. Griffin, A. S. & West, S. A. Kin discrimination and the benefit of helping in cooperatively breeding vertebrates. *Science* **302**, 634–636 (2003).
9. Velicer, G. J. Social strife in the microbial world. *Trends Microbiol.* **11**, 330–337 (2003).
10. Queller, D. C. & Strassmann, J. E. Kin selection and social insects. *Bioscience* **48**, 165–175 (1998).
11. Queller, D. C. Genetic relatedness in viscous populations. *Evol. Ecol.* **8**, 70–73 (1994).

12. West, S. A., Pen, I. & Griffin, A. S. Cooperation and competition between relatives. *Science* **296**, 72–75 (2002).
13. Taylor, P. D. Altruism in viscous populations - an inclusive fitness model. *Evol. Ecol.* **6**, 352–356 (1992).
14. Wilson, D. S., Pollock, G. B. & Dugatkin, L. A. Can altruism evolve in purely viscous populations. *Evol. Ecol.* **6**, 331–341 (1992).
15. Guerinet, M. L. Microbial iron transport. *Annu. Rev. Microbiol.* **48**, 743–772 (1994).
16. Ratledge, C. & Dover, L. G. Iron metabolism in pathogenic bacteria. *Annu. Rev. Microbiol.* **54**, 881–941 (2000).
17. West, S. A. & Buckling, A. Cooperation, virulence and siderophore production in bacterial parasites. *Proc. R. Soc. Lond. B* **270**, 37–44 (2003).
18. Brown, S. P. Cooperation and conflict in host-manipulating parasites. *Proc. R. Soc. Lond. B* **266**, 1899–1904 (1999).
19. Brown, S. P., Hochberg, M. E. & Grenfell, B. T. Does multiple infection select for raised virulence? *Trends Microbiol.* **10**, 401–405 (2002).
20. Grafen, A. In *Behavioural Ecology: An Evolutionary Approach* (eds Krebs, J. R. & Davies, N. B.) 62–84 (Blackwell Scientific Publications, Oxford, 1984).
21. Frank, S. A. Models of parasite virulence. *Q. Rev. Biol.* **71**, 37–78 (1996).
22. West, S. A., Murray, M. G., Machado, C. A., Griffin, A. S. & Herre, E. A. Testing Hamilton's rule with competition between relatives. *Nature* **409**, 510–513 (2001).
23. Velicer, G. J. & Yu, Y. N. Evolution of novel cooperative swarming in the bacterium *Myxococcus xanthus*. *Nature* **425**, 75–78 (2003).
24. Rainey, P. B. & Rainey, K. Evolution of cooperation and conflict in experimental bacterial populations. *Nature* **425**, 72–74 (2003).
25. Pepper, J. W. Relatedness in trait group models of social evolution. *J. Theor. Biol.* **206**, 355–368 (2000).
26. De Vos, D. et al. Study of pyoverdinin type and production by *Pseudomonas aeruginosa* isolated from cystic fibrosis patients: prevalence of type II pyoverdinin isolates and accumulation of pyoverdinin-negative mutants. *Arch. Microbiol.* **175**, 384–388 (2001).
27. Meyer, J. M., Neely, A., Stintzi, A., Georges, C. & Holder, I. A. Pyoverdinin is essential for virulence of *Pseudomonas aeruginosa*. *Infect. Immun.* **64**, 518–523 (1996).
28. Strassmann, J. E., Zhu, Y. & Queller, D. C. Altruism and social cheating in the social amoeba *Dictyostelium discoideum*. *Nature* **408**, 965–967 (2000).
29. Gandon, S., Mackinnon, M. J., Nee, S. & Read, A. F. Imperfect vaccines and the evolution of pathogen virulence. *Nature* **414**, 751–756 (2002).
30. Hoogkamp-Korstanje, J. A. A., Meis, J. F. G. M., Kissing, J., van der Laag, J. & Melchers, W. J. G. Risk of cross-colonization and infection by *Pseudomonas aeruginosa* in a holiday camp for cystic fibrosis patients. *J. Clin. Microbiol.* **33**, 572–575 (1995).

Acknowledgements We thank J.-M. Meyer for supplying strains; A. Gardner and D. Shuker for discussion and comments; A. Duncan and A. Graham for laboratory assistance; staff at the Bega Public Library, NSW, Australia, for internet access; BBSRC, NERC and Royal Society for funding.

Competing interests statement The authors declare that they have no competing financial interests.

Correspondence and requests for materials should be addressed to A.S.G. (a.griffin@ed.ac.uk).

High rates of N₂ fixation by unicellular diazotrophs in the oligotrophic Pacific Ocean

Joseph P. Montoya¹, Carolyn M. Holl¹, Jonathan P. Zehr², Andrew Hansen³, Tracy A. Villareal⁴ & Douglas G. Capone⁵

¹School of Biology, Georgia Institute of Technology, Atlanta, Georgia 30332, USA

²Department of Ocean Sciences and Institute of Marine Science, University of California, Santa Cruz, California 95064, USA

³School of Ocean and Earth Science and Technology, University of Hawaii, Honolulu, Hawaii 96822, USA

⁴Marine Science Institute, The University of Texas at Austin, Port Aransas, Texas 78373, USA

⁵Department of Biological Sciences and The Wrigley Institute for Environmental Studies, University of Southern California, Los Angeles, California 90089, USA

The availability of nitrogen is important in regulating biological productivity in marine environments. Deepwater nitrate has long been considered the major source of new nitrogen supporting primary production in oligotrophic regions of the open ocean, but recent studies have showed that biological N₂ fixation has a critical role in supporting oceanic new production^{1–7}. Large colonial cyanobacteria in the genus *Trichodesmium* and the

heterocystous endosymbiont *Richelia* have traditionally been considered the dominant marine N₂ fixers, but unicellular diazotrophic cyanobacteria and bacterioplankton have recently been found in the picoplankton and nanoplankton community of the North Pacific central gyre, and a variety of molecular and isotopic evidence suggests that these unicells could make a major contribution to the oceanic N budget⁸. Here we report rates of N₂ fixation by these small, previously overlooked diazotrophs that, although spatially variable, can equal or exceed the rate of N₂ fixation reported for larger, more obvious organisms. Direct measurements of ¹⁵N₂ fixation by small diazotrophs in various parts of the Pacific Ocean, including the waters off Hawaii where the unicellular diazotrophs were first characterized, show that N₂ fixation by unicellular diazotrophs can support a significant fraction of total new production in oligotrophic waters.

The recent discovery of N₂-fixing coccoid cyanobacteria and bacteria in the North Pacific subtropical gyre⁸ revealed a potentially important source of new nitrogen to support oceanic production, but the small size and low numeric abundance of these organisms⁸ pose significant challenges for quantifying their N₂ fixation activity. We applied a high-sensitivity tracer technique⁹ to measure the rate of N₂ fixation by the small size fraction (less than 10 μm) of plankton from an extensive region of subtropical and tropical waters in the Pacific. In contrast to two recent studies that documented measurable but low rates of N₂ fixation by small

diazotrophs at or near the Hawaii Ocean Timeseries station ALOHA north of Oahu^{10,11}, our data provide the first spatially extensive direct measurements of N₂ fixation by small diazotrophs in oligotrophic waters and show that these recently discovered organisms can make a major contribution to oceanic N₂ fixation.

Experiments performed across broad expanses of the eastern North Pacific and waters north of Australia show that the rate of ¹⁵N₂ fixation by the unicellular diazotroph size fraction is measurable, and at times very high (Fig. 1). Our most intensive experiments were performed with water collected at 25 m depth at ALOHA, or from the surface outside Kaneohe bay, Oahu. In all these experiments, we found N₂ fixation by small diazotrophs at rates of 0.01–0.15 nmol N l⁻¹ h⁻¹ (Fig. 2a), with the highest rates in August 2001 and February 2002. By integrating our rates through the water column (see Methods), we calculated areal rates of N₂ fixation between 11 and 103 μmol N m⁻² d⁻¹ with a mean of 66 ± 19 μmol N m⁻² d⁻¹ (N = 7). Although we conservatively assumed only 12 h of daily N₂ fixation activity, our data do not show any consistent temporal phasing of N₂ fixation activity, and N₂ fixation seems to occur during the day as well as at night. This result contrasts sharply with the obligate diel pattern in N₂ fixation activity by *Trichodesmium*^{12,13}, and the apparent dominance of night-time acetylene reduction in highly concentrated samples taken near station ALOHA¹¹.

The volumetric rates of N₂ fixation that we measured for ALOHA

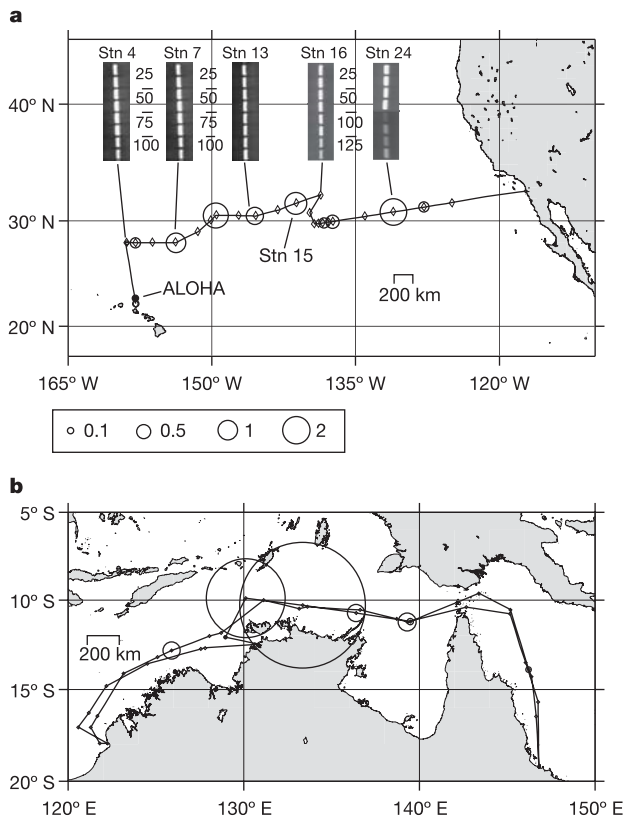


Figure 1 Volumetric rate of N₂ fixation by unicellular organisms in the North Pacific Ocean and near Australia. The area of each circle is proportional to the N₂ fixation rate as shown (in nmol N l⁻¹ h⁻¹). Stations where no rate measurements were made are marked with diamonds. **a**, N₂ fixation rates measured at ALOHA and during cruise Cook-25 (Jun - Jul 2002). Insets show occurrence of *nifH* (bands) as a function of depth in metres at selected stations. At all depths, clone libraries constructed by amplification with degenerate *nifH* primers were dominated by group A cyanobacterial sequences. **b**, Rates measured during cruise EW9912 (October to November 1999). Charts prepared using the Generic Mapping Tools^{20,21}.

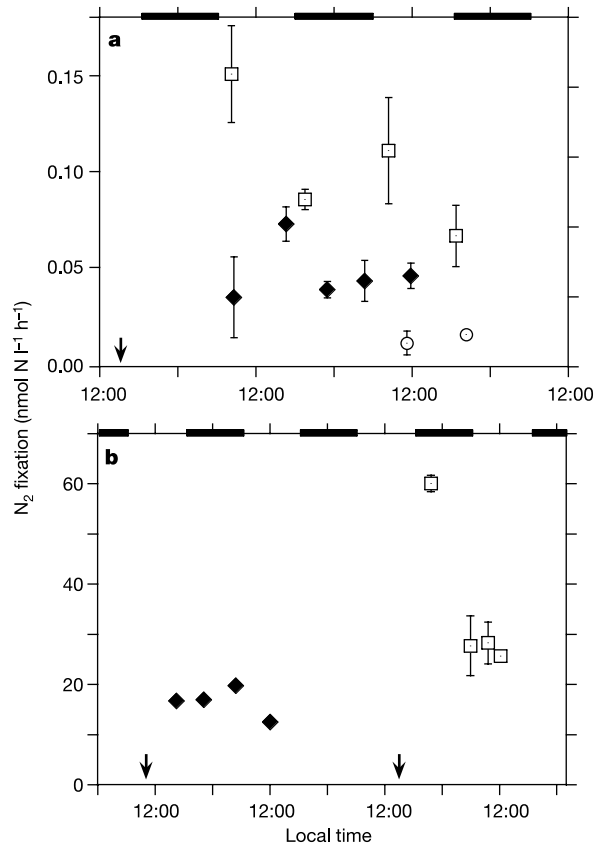


Figure 2 Time course of N₂ fixation in incubations under simulated *in situ* conditions. Each symbol represents the integrated rate of N₂ fixation between the start (arrow) and the endpoint of an incubation. **a**, Experiments performed in July 2000 (circles) and August 2001 (squares) with water from 25 m at ALOHA and an experiment performed in February 2002 (diamonds) with water collected just outside Kaneohe bay. Results are means ± s.d. for three replicates. **b**, Experiments at two stations in the Arafura Sea using water from the subsurface pigment maximum (50–60 m). Results are means ± s.d. for two replicates.

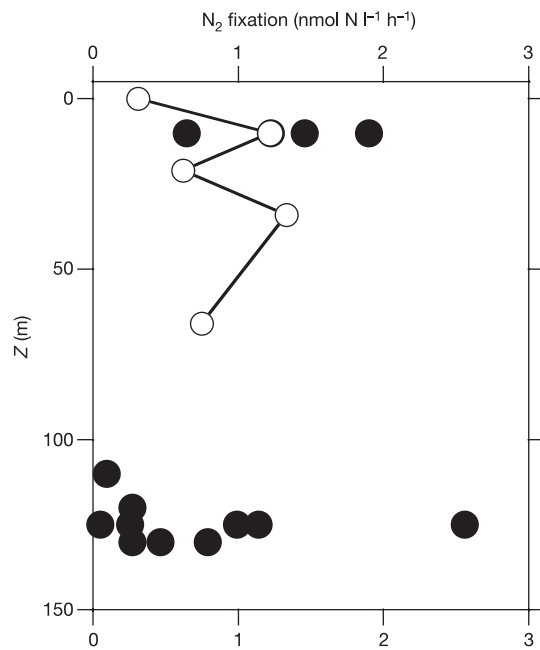


Figure 3 Summary of rate measurements as a function of depth at stations along a transect in the eastern subtropical Pacific from Hawaii to San Diego (cruise Cook-25). At station 15 (31° 32.21' N, 141° 15.66' W), N₂ fixation was measured in water samples from five different depths through the mixed layer (open circles). At other stations, N₂ fixation was measured in water collected either from the subsurface pigment maximum or from about 10 m depth (filled circles).

are substantially higher than those previously reported for the same waters^{10,11}. This contrast might reflect differences in experimental approach and sample handling as well as real temporal variation in N₂ fixation activity in this region. Nitrogenase gene sequences of two distinct groups of unicellular cyanobacteria have previously been detected in the Pacific Ocean at station ALOHA⁸. One group, designated group A, has yet to be fully characterized, whereas the group B sequence type is closely related to cultivated strains of marine *Synechocystis* (*Crocospaera*). Group A diazotrophic cyanobacteria sequence types were recovered from messenger RNA in all experiments with water from station ALOHA. Direct cell counts revealed *Synechocystis*-like cells (that is, potential diazotrophs 3–7 μm in diameter, compared with smaller synechococoids and prochlorococoids) at concentrations of 5–10 cells ml⁻¹ in July 2000 and up to 200 cells ml⁻¹ in our August 2001 experiment. These differences in *Synechocystis*-like cell abundance are large enough to account for the range of variation that we observed in N₂ fixation rate at ALOHA.

We also performed a series of experiments and diazotroph diversity measurements along a cruise track through the eastern North Pacific from Hawaii to California (Fig. 1a), along which we measured N₂ fixation in water from the mixed layer and subsurface pigment maximum to assess the spatial distribution of diazotrophy across a significant expanse of subtropical waters. On this transect, the maximal pigment concentrations typically occurred near the base of the mixed layer at about 120 m depth, although several stations in a bloom of large diatoms (*Rhizosolenia* and *Hemiaulus*) had shallow pigment maxima at about 10 m depth. At all 11 stations where we performed rate measurements, we found measurable N₂ fixation activity in the pigment maximum, ranging between 0.047 and 1.85 nmol N l⁻¹ h⁻¹, with an overall mean of 0.72 ± 0.20 nmol N l⁻¹ h⁻¹ (N = 11). Most of the rates measured on this

Table 1 Summary of N₂ fixation estimates for oligotrophic waters

| Location/domain | Dates | Mean areal rate (μmol N m ⁻² d ⁻¹) | S.e.m. | N | Notes |
|---|----------------|---|--------|-----|--|
| Direct rate measurements | | | | | |
| Unicellular diazotrophs | | | | | |
| ALOHA ¹⁰ | 2000–2001 | 24 | 6 | 3 | ¹⁵ N ₂ uptake integrated over 100 m |
| ALOHA region ¹¹ | Autumn 2002 | 2.2 | | 1 | AR in pre-concentrated (130–160 ×) water samples |
| ALOHA (this study) | 2000–2001 | 66 | 19 | 7 | ¹⁵ N ₂ uptake; 77% of the rate at 25 m integrated over 100 m; see text for additional details |
| Kaneohe bay (this study) | 2000–2002 | 24 | 6 | 12 | ¹⁵ N ₂ uptake integrated over 25 m |
| Eastern North Pacific gyre (this study) | June–July 2002 | 520 | 160 | 10 | ¹⁵ N ₂ uptake integrated through the mixed layer and excluding one high outlier (3,830 μmol N m ⁻² d ⁻¹ at station 24) |
| Timor–Arafura–Coral seas (this study) | Nov. 1999 | 126 | 47 | 7 | ¹⁵ N ₂ uptake integrated through the mixed layer and excluding stations 26 and 27 |
| Arafura Sea (this study) | Nov. 1999 | 3,955 | | 2 | ¹⁵ N ₂ uptake in the pigment maximum, stations 26 and 27 |
| <i>Trichodesmium</i> | | | | | |
| Southwestern N Atlantic ²² 0–24° N, 45–66° W | Nov. 1964 | 41 | 7.6 | 19 | ¹⁵ N ₂ uptake |
| | May 1965 | 108 | 24 | 17 | |
| Caribbean ²³ , 12–22° N | | 161 | 20 | 12 | AR |
| BATS ²⁴ | 1995–1997 | 41 | | 14 | ¹⁵ N ₂ uptake |
| N Atlantic | 1995–2001 | 254 | 40 | 155 | AR (D.G.C., J. A. Burns, J.P.M., A. F. Michaels, A. Subramaniam and E. J. Carpenter, unpublished data) |
| N Pacific ²⁵ , 21° N, 159° W | 1972 | 134 | | 2 | AR |
| East China Sea ²⁶ , 10–25° N | | 126 | 49 | 32 | AR |
| HOT/ALOHA ⁵ | 1990–1992 | 84 | 43 | 8 | AR |
| Arabian Sea ²⁷ , 7–10° N | May 1995 | 35 | 7.4 | 9 | AR |
| Arabian Sea ²⁷ , 10° N bloom | May 1995 | 99 | 25 | 5 | AR, upper 0.5 m |
| <i>Richelia/Hemiaulus</i> | | | | | |
| SW N Atlantic ²⁸ , 7–27° N | Oct. 1996 | 3,110 | 1,315 | 14 | AR |
| Geochemical budgets and mass balances | | | | | |
| N Atlantic ⁴ | | 500–2,500 | | | Based on N* distributions |
| N Atlantic ² | | 197 | | | Based on N* distributions |
| Atlantic ¹⁴ , 40° N to 40° S | | 48 | | | Based on dissolved inorganic C inventory |
| Pacific ¹⁴ , 40° N to 40° S | | 137 | | | Based on dissolved inorganic C inventory |
| Pacific ²⁹ | | 97 | | | Total rate (59 Tg N yr ⁻¹) based on N* distributions; Areal rate calculated for region between 40° N and 40° S. |
| HOT/ALOHA ⁵ | | 93 | 38 | | Based on N:P stoichiometry |
| HOT/ALOHA ¹⁰ | | 135 | 15 | 11 | Based on ¹⁵ N mass balance |

HOT, Hawaii Ocean Timeseries. BATS, Bermuda Atlantic Timeseries station. N* is a quantitative measure of N:P ratio anomalies relative to oceanic averages. Rate estimates are based on direct measurements as well as geochemical budgets. Acetylene reduction (AR) estimates are based on a 3:1 reduction ratio for conversion to N₂ fixation rates.

transect (Figs 1a and 3) were substantially higher than at ALOHA (Table 1). Although this cruise occurred in a different year from our ALOHA experiments, the rate we measured at the station nearest ALOHA was quite similar to the mean of the rates measured in our focused experiments with ALOHA water (Fig. 1a). Thus, N_2 fixation rates by unicellular diazotrophs might be much higher elsewhere in the basin, and N_2 fixation rates at ALOHA might not be representative of the entire subtropical gyre.

Our rate measurements from this cruise generally focused on a single depth at each station, although we successfully amplified *nifH* DNA sequences throughout the mixed layer of all stations assayed for diazotroph diversity (Fig. 1a). As at ALOHA, our clone libraries from this cruise track were dominated by group A cyanobacterial sequences, whereas bacterial sequences composed only about 1% of the community. The areal rate of N_2 fixation ranged between 70 and 2,800 $\mu\text{mol N m}^{-2} \text{d}^{-1}$. Excluding the one extreme value, the overall mean for the entire transect was $520 \pm 160 \mu\text{mol N m}^{-2} \text{d}^{-1}$ ($N = 10$). In comparison, estimates of the average rate of injection of deepwater NO_3^- into the mixed layer of the oligotrophic North Pacific span a range of about 150–1100 $\mu\text{mol N m}^{-2} \text{d}^{-1}$ (refs 10, 14, 15) in the central gyre to 3600 $\mu\text{mol N m}^{-2} \text{d}^{-1}$ in the equatorial upwelling region¹⁶. This implies that N_2 fixation by small plankton can support a substantial fraction of total new production in the North Pacific and might be comparable to deepwater NO_3^- as a source of new nitrogen to the euphotic zone. The very highest rates of N_2 fixation that we measured could potentially supply new nitrogen to the upper water column at a rate comparable to that of the equatorial upwelling system, although without any accompanying PO_4^{3-} to support the balanced growth of plankton.

Experiments performed on a cruise north of Australia complement our North Pacific data (Fig. 2b). In this shallow shelf system we found measurable N_2 fixation by small diazotrophs at all stations where we conducted rate measurements (Fig. 1b). In particular, extremely high N_2 fixation rates were found in the pigment maximum (50–60 m) in the Arafura Sea. In two experiments performed on successive days, we measured average rates of N_2 fixation of 20–30 $\text{nmol N l}^{-1} \text{h}^{-1}$ and as high as 62 $\text{nmol N l}^{-1} \text{h}^{-1}$. The latter value is the highest rate we have ever measured in a natural sample and occurred in a 7-h incubation extending from mid-afternoon into the evening (14:00 to 21:00 local) of the second day of this study (Fig. 2b). As at ALOHA, the rate of N_2 fixation in these two Arafura Sea experiments could turn over the standing stock of nitrogen in the pigment maximum on a timescale of 1–4 days.

We calculated a mean areal rate of N_2 fixation in the mixed layer of 126 $\mu\text{mol N m}^{-2} \text{d}^{-1}$ for locations other than our two high-rate stations in the Arafura Sea (see Methods). This is roughly a quarter of the mean rate that we measured for our North Pacific transect. In contrast, at our two high-activity stations in the Arafura Sea, we calculated an areal rate of N_2 fixation in the pigment maximum proper of almost 4 $\text{mmol N m}^{-2} \text{d}^{-1}$ (Fig. 1b, Table 1).

Unlike *Trichodesmium*, which resides in the shallower portions of the upper euphotic zone¹⁷, unicellular diazotrophs seem more uniformly distributed through the water column (Fig. 1a), and our experiments show clear evidence for significant N_2 fixation by unicells in diverse parts of the Pacific Ocean. Our rates are substantially higher than reported previously for unicellular diazotrophs (Table 1), a contrast that might reflect both spatial/temporal variability and differences in experimental detail^{10,11}. In addition, the errors likely to arise in $^{15}\text{N}_2$ tracer incubations (for example, loss of tracer from the incubation vessel and leakage of fixed nitrogen from cells during filtration) are asymmetric in effect and tend to produce underestimates of the true rate⁹. In sum, our results indicate a major flux of new nitrogen entering oceanic systems in addition to that due to large diazotrophs alone. Moreover, *Trichodesmium* has very few known grazers⁶, so the pathways by

which recently fixed nitrogen enters higher trophic levels might also be distinct for these two groups of marine diazotrophs. Our observations support a fundamental change in our estimates of the rate and mechanisms of nutrient supply to the oligotrophic ocean. Our conservative estimates (for example, assuming only 12 h of activity per day) of the mean N_2 fixation rate by small diazotrophs in the North Pacific, extrapolated over the region with mean annual surface temperature of more than 25 °C (about $29 \times 10^{12} \text{m}^2$), could support new production of roughly 0.4Pg C yr^{-1} , which is about 10% of recent estimates of total oceanic new production¹⁴. N_2 fixation by unicellular diazotrophs might be the largest flux of new nitrogen into the upper water column of the oligotrophic Pacific, and perhaps other such waters. □

Methods

Rate measurements

We collected water samples for N_2 fixation assays at the Hawaii Ocean Timeseries station ALOHA, in the waters north of Australia (cruise EW-9912) and along a transect from Hawaii to San Diego (cruise Cook-25). All water samples were passed through 100- μm Nitex mesh before incubation to exclude large organisms, including *Trichodesmium* colonies and large diatoms such as *Hemiaulus* that might contain endosymbiotic N_2 fixers. Measurements of N_2 fixation rate were performed in 4-l polycarbonate bottles equipped with silicone septum caps to which trace additions of $^{15}\text{N}_2$ (99 atom%; Cambridge Isotope) were made with a gas-tight syringe.

For experiments in Hawaii, water was collected either at 25 m depth at ALOHA during routine Hawaii Ocean Timeseries cruises with the use of a CTD-rosette sampling system or at the surface just outside Kaneohe bay, Oahu. Once collected, water samples were transported in 50-l polycarbonate bottles to the Hawaii Institute of Marine Biology on Coconut Island, Kaneohe bay. Once there, the sample was transferred to 4-l incubation bottles for rate measurements. All experimental incubations were run in triplicate and terminated in a time series extending 36–48 h.

During cruises EW9912 (October to November 1997) and Cook-25 (June to July 2002), water samples were collected from the mixed layer and pigment maximum with the use of a CTD-rosette system and were incubated on deck for 24–36 h.

Incubations were terminated by gentle pressure filtration through a precombusted GF/F filter after passage through a 10- μm prefilter to remove larger phytoplankton from the sample. Sample filters were dried at 60 °C, then stored over desiccant until analysed by continuous-flow isotope ratio mass spectrometry with a Micromass Optima mass spectrometer interfaced to a CE Elantech NA2500 elemental analyser.

Areal rate calculations

At most stations we made N_2 fixation measurements at one or several depths and took different approaches to integrating these rates through the water column to estimate the areal rate of N_2 fixation. In experiments carried out at ALOHA¹⁰, the rate of N_2 fixation decreased with depth such that the average rate in the upper 100 m of the water column was about 77% of the rate measured at 25 m. We used this scaling factor (77%) to estimate the areal rate of N_2 fixation implied by our rate measurements at 25 m depth at ALOHA.

We took a more conservative approach in estimating areal fluxes by using measurements from our cruises in the North Pacific and Australian waters. In both cases, our data generally focused on a single depth at each station, typically in the subsurface pigment maximum at 50–100 m. A profile of rate measurements made at station 15 near the middle of the North Pacific transect showed rates of 0.31–1.3 $\text{nmol N l}^{-1} \text{h}^{-1}$ with a mean of 0.85 ± 0.21 ($N = 5$) and little obvious vertical structure (Fig. 3). These rates agree well with the range of values measured in the pigment maximum elsewhere on the transect (Fig. 3), indicating that our measurements in the pigment maximum should be representative of the mixed layer as a whole. While recognizing that vertically resolved rate measurements at all stations would be preferable, we conservatively estimated the areal rate of N_2 fixation on these cruises by assuming that N_2 fixation was uniform through the mixed layer rather than highest at the surface. We then integrated our volumetric rates through the mixed layer and assumed, again conservatively, that N_2 fixation occurs for only 12 h d^{-1} . For the two Arafura Sea stations with extremely high rates of N_2 fixation in the pigment maximum, we performed our rate integration through the pigment maximum alone (10 m), rather than through the entire mixed layer.

Where confidence intervals are given, results are means \pm s.e.m.

Diazotroph diversity

Water samples were collected for molecular characterization of the diazotroph community at ALOHA and at selected stations on the Cook-25 cruise. One-litre seawater samples from each depth were filtered on 0.2 μm pore-size Supor filters (Pall Gelman Inc., Ann Arbor, Michigan). The filters were placed in 2-ml centrifuge tubes containing 500 μl of 1 \times Tris-EDTA buffer (10 mM Tris-HCl at pH 7.4 and 1 mM EDTA at pH 8.0). Centrifuge tubes were immediately frozen in liquid nitrogen and transported to the shore-based laboratory for analyses.

Nucleic acids were extracted with the protocol described by Tillett and Neilan¹⁸. DNA concentrations in the extracts were quantified by PicoGreen DNA quantification (Molecular Probes, Eugene, Oregon) with a spectral fluorimeter in accordance with the manufacturer's specifications. To assess the diversity of *nifH*-containing plankton at

station ALOHA, samples were amplified by polymerase chain reaction (PCR) with a nested set of degenerate *nifH* primers^{19,20}. The resulting PCR products were cloned and sequenced to characterize the *nifH* sequence diversity. Detailed descriptions of the methods used for the PCR amplification, cloning and sequencing are found in ref. 19.

Received 18 May; accepted 8 July 2004; doi:10.1038/nature02824.

1. Carpenter, E. J. & Romans, K. Major role of the cyanobacterium *Trichodesmium* in nutrient cycling in the North Atlantic Ocean. *Science* **254**, 1356–1358 (1991).
2. Gruber, N. & Sarmiento, J. L. Global patterns of marine nitrogen fixation and denitrification. *Glob. Biogeochem. Cycles* **11**, 235–266 (1997).
3. Lipschultz, F. & Owens, N. J. P. An assessment of nitrogen fixation as a source of nitrogen to the North Atlantic Ocean. *Biogeochemistry* **35**, 261–274 (1996).
4. Michaels, A. F. *et al.* Inputs, losses and transformations of nitrogen and phosphorus in the pelagic North Atlantic Ocean. *Biogeochemistry* **35**, 181–226 (1996).
5. Karl, D. *et al.* The role of nitrogen fixation in biogeochemical cycling in the subtropical North Pacific Ocean. *Nature* **388**, 533–538 (1997).
6. Capone, D. G., Zehr, J. P., Paerl, H. W., Bergman, B. & Carpenter, E. J. *Trichodesmium*, a globally significant marine cyanobacterium. *Science* **276**, 1221–1229 (1997).
7. Montoya, J. P., Carpenter, E. J. & Capone, D. G. Nitrogen-fixation and nitrogen isotope abundances in zooplankton of the oligotrophic North Atlantic. *Limnol. Oceanogr.* **47**, 1617–1628 (2002).
8. Zehr, J. P. *et al.* Unicellular cyanobacteria fix N₂ in the subtropical North Pacific Ocean. *Nature* **412**, 635–638 (2001).
9. Montoya, J. P., Voss, M., Kaehler, P. & Capone, D. G. A simple, high precision, high sensitivity tracer assay for dinitrogen fixation. *Appl. Environ. Microbiol.* **62**, 986–993 (1996).
10. Dore, J. E., Brum, J. R., Tupas, L. & Karl, D. M. Seasonal and interannual variability in sources of nitrogen supporting export in the oligotrophic subtropical North Pacific Ocean. *Limnol. Oceanogr.* **47**, 1595–1607 (2002).
11. Falcon, L. I., Carpenter, E. J., Cipriano, F., Bergman, B. & Capone, D. G. N₂ fixation by unicellular bacterioplankton from the Atlantic and Pacific Oceans: Phylogeny and in situ rates. *Appl. Environ. Microbiol.* **70**, 765–770 (2004).
12. Capone, D. G., O'Neil, J. M., Zehr, J. & Carpenter, E. J. Basis for diel variation in nitrogenase activity in the marine planktonic cyanobacterium *Trichodesmium thiebautii*. *Appl. Environ. Microbiol.* **56**, 3532–3536 (1990).
13. Chen, Y.-B., Zehr, J. P. & Mellon, M. T. Growth and nitrogen fixation of the diazotrophic filamentous nonheterocystous cyanobacterium *Trichodesmium* sp. IMS101 in defined media: evidence for a circadian rhythm. *J. Phycol.* **32**, 916–923 (1996).
14. Lee, K., Karl, D. M., Wanninkhof, R. H. & Zhang, J. Z. Global estimates of net carbon production in the nitrate-depleted tropical and subtropical oceans. *Geophys. Res. Lett.* **29** (2002) doi: 10.1029/2001GL014198.
15. Allen, C. B., Kanda, J. & Laws, E. A. New production and photosynthetic rates within and outside a cyclonic mesoscale eddy in the North Pacific subtropical gyre. *Deep-Sea Res.* **143**, 917–936 (1996).
16. Aufdenkampe, A. K. *et al.* Biogeochemical controls on new production in the tropical Pacific. *Deep-Sea Res.* **49**, 2619–2648 (2002).
17. Carpenter, E. J., Subramaniam, A. & Capone, D. G. Biomass and productivity of the cyanobacterium, *Trichodesmium* spp. in the tropical North Atlantic Ocean. *Deep-Sea Res.* **51**, 173–203 (2004).
18. Tillett, D. & Neilan, B. A. Xanthogenate nucleic acid isolation from cultured and environmental cyanobacteria. *J. Phycol.* **36**, 251–258 (2004).
19. Zehr, J. P. & Turner, P. J. in *Methods in Marine Microbiology* (ed. Paul, J. H.) 271–286 (Academic, San Diego, 2001).
20. Zehr, J. P. & McReynolds, L. A. Use of degenerate oligonucleotides for amplification of the *nifH* gene from the marine cyanobacterium *Trichodesmium thiebautii*. *Appl. Environ. Microbiol.* **55**, 2522–2526 (1989).
21. Wessel, P. & Smith, W. H. F. New, improved version of Generic Mapping Tools released. *Eos* **79**, 579 (1998).
22. Goering, J. J., Dugdale, R. C. & Menzel, D. W. Estimate of in situ rates of nitrogen uptake by *Trichodesmium* sp. in the Tropical Atlantic Ocean. *Limnol. Oceanogr.* **11**, 614–620 (1966).
23. Carpenter, E. J. & Price, C. C. Nitrogen fixation, distribution and production of *Oscillatoria* (*Trichodesmium*) spp. in the western Sargasso and Caribbean Seas. *Limnol. Oceanogr.* **22**, 60–72 (1977).
24. Orcutt, K. M. *et al.* A seasonal study of the significance of N₂ fixation by *Trichodesmium* spp. at the Bermuda Atlantic Time-series Study (BATS) site. *Deep-Sea Res.* **48**, 1583–1608 (2001).
25. Gundersen, K. R. *et al.* Structure and biological dynamics of the oligotrophic ocean photic zone off the Hawaiian Islands. *Pacif. Sci.* **30**, 45–68 (1976).
26. Saino, T. *Biological Nitrogen Fixation in the Ocean with Emphasis on the Nitrogen Fixing Blue-Green Alga, Trichodesmium, and its Significance in the Nitrogen Cycle in the Low Latitude Sea Areas* (Univ. Tokyo, Tokyo, 1977).
27. Capone, D. G. *et al.* An extensive bloom of the N₂-fixing cyanobacterium, *Trichodesmium erythraeum*, in the central Arabian Sea. *Mar. Ecol. Prog. Ser.* **172**, 281–292 (1998).
28. Carpenter, E. J. *et al.* Extensive bloom of a N₂-fixing diatom/cyanobacterial association in the tropical Atlantic Ocean. *Mar. Ecol. Prog. Ser.* **185**, 273–283 (1999).
29. Deutsch, C. *et al.* Denitrification and N₂ fixation in the Pacific Ocean. *Glob. Biogeochem. Cycles* **15**, 483–506 (2001).

Acknowledgements We thank D. Karl and the entire HOT team for support in Hawaii; A. Gibson for collecting samples for molecular characterization on cruise Cook-25; C. Payne, K. Rathbun, S. Patel, K. Ghanouni, P. Davoodi and G. Stewart for their assistance in the laboratory analyses; and the captains and crews of the RV *Ewing* and RV *Melville* for their assistance at sea. This research was supported by grants from the National Science Foundation.

Competing interests statement The authors declare that they have no competing financial interests.

Correspondence and requests for materials should be addressed to J.P.M. (j.montoya@biology.gatech.edu).

Control of phyllotaxy by the cytokinin-inducible response regulator homologue *ABPHYL1*

Anna Giulini*, Jing Wang & David Jackson

Cold Spring Harbor Laboratory, 1 Bungtown Road, Cold Spring Harbor, New York 11724, USA

* Present address: Department of Plant Production, University of Milan, Via Celoria 2, 20133 Milan, Italy

Phyllotaxy describes the geometric pattern of leaves and flowers, and has intrigued botanists and mathematicians for centuries^{1,2}. How these patterns are initiated is poorly understood, and this is partly due to the paucity of mutants³. Signalling by the plant hormone auxin appears to determine the site of leaf initiation; however, this observation does not explain how distinct patterns of phyllotaxy are initiated⁴. *abphyl1* (*abph1*) mutants of maize initiate leaves in a decussate pattern (that is, paired at 180°), in contrast to the alternating or distichous phyllotaxy observed in wild-type maize and other grasses⁵. Here we show that *ABPH1* is homologous to two-component response regulators and is induced by the plant hormone cytokinin. *ABPH1* is expressed in the embryonic shoot apical meristem, and its spatial expression pattern changes rapidly with cytokinin treatment. We propose that *ABPH1* controls phyllotactic patterning by negatively regulating the cytokinin-induced expansion of the shoot meristem, thereby limiting the space available for primordium initiation at the apex.

Named after their ability to promote proliferation of cultured cells, the cytokinins have diverse roles in shoot morphogenesis^{6,7}. Cytokinin signals are perceived by trans-membrane histidine kinase receptors, which regulate gene expression through transcription factors known as response regulators (reviewed in refs 8, 9). Although the molecular details of this pathway have been described in detail, the precise biological functions of the response regulators are unknown, as loss-of-function mutants do not have striking phenotypes^{10–13}. Here we show that the phyllotaxy mutant *abph1* is caused by a loss-of-function mutation in a cytokinin-inducible response regulator.

abph1 mutants can have opposite leaf (decussate) phyllotaxy throughout their life cycle, and also initiate ears in opposite pairs (Fig. 1a, b). The altered phyllotaxy originates at the shoot apical meristem (SAM) by the initiation of leaf primordia in opposite pairs (Fig. 1c, d)^{5,14}. Our reference *abph1* allele, *abph1-0*, arose spontaneously in breeding stocks⁵. We screened for putative tagged alleles in progeny from crosses of mutant plants onto *Mutator* (*Mu*) or *Suppressor-mutator* transposon lines, and recovered four novel alleles. Co-segregation analysis using one of the *Mu* alleles, *abph1-mum181*, identified a 4-kilobase (kb) *Mu7* hybridizing band in 50 mutant individuals but not in any wild-type siblings or progenitors (not shown). We cloned this band from a sub-genomic library, and amplified the flanking sequences by polymerase chain reaction (PCR). The products contained an entire open reading frame arranged in five predicted exons, with the *Mu7* transposon 3 bp downstream of the predicted start codon (Fig. 1e).

We used this candidate gene as a probe to characterize additional *abph1* alleles. Southern blotting revealed that the three other transposon alleles were deleted for the cloned flanking region (Supplementary Fig. S1b); *Mu* transposons are known to give rise to deletions¹⁵. We were unable to amplify the intact coding region from the *abph1-0* reference allele (supplementary data, Fig. S1d) or to detect transcript from this allele on northern blots (not shown) or by PCR with reverse transcriptase (RT-PCR) (Fig. 2a). We obtained